

# The Influence of Bat Wings For Producing Efficient Net Body Forces in Bio-inspired Flapping Robots

Julian Colorado<sup>1</sup>, Claudio Rossi<sup>2</sup>, Antonio Barrientos<sup>2</sup> and Diego Patino<sup>1</sup>

<sup>1</sup>*School of Engineering, Pontificia Universidad Javeriana, Cr. 7 No. 40-62, Bogotá, Colombia*

<sup>2</sup>*Centre for Automation and Robotics, Universidad Politécnica de Madrid, C/ José Abascal 2, 28006, Madrid, Spain*

**Keywords:** Bio-inspired MAV, Shape Memory Alloy Actuators, Bats.

**Abstract:** Bat wings contain dozens of joints that enable the animal to perform aggressive maneuvers by means of changing the wing shape during flight. There is evidence that the inertial forces produced by their wings during flapping have a key role in the attitude movements of the animal, i.e. aerial rotations. In fact, bats efficiently generate net body forces to manoeuvre by taking advantage of their large wing-to-body mass ratio. In this paper, the following question is formulated: *Could a Micro Aerial Vehicle (MAV) inspired by the biomechanics of bats take advantage of the morphing-wings aimed at increasing net body forces?* Using BaTbot, a novel bat-like MAV with highly articulated wings actuated by shape memory alloy actuators, our goal is to quantify the effects of different wing modulation patterns on the generation of net body forces. Experiments are carried out to confirm the important physical role that changing the wing shape enables: the contraction time of the wings (upstroke) should be faster than the extension time (downstroke), taking about 37.5% of the wingbeat period. This modulation pattern has enabled a lift force increment of 22% (from  $L = 0.92N$  to  $L = 1.12N$ ), abrupt drag reduction (from  $D = 0.22N$  to  $D = 0.11N$ ) and also an increase of net body forces ( $F_{net}$ ) about 28% compared to those wing modulation patterns defined with equal periods for contraction/extension. These findings can be useful for accurate dynamics modelling and efficient design of flight controllers applied to morphing-wing micro aerial vehicles.

## 1 INTRODUCTION

Morphing-wing aircrafts have emerged as a direction to enhance the efficiency of flight by changing the wing profile (Gomez and Garcia, 2011). There is a growing interest in the energy cost of flight and learning from nature is the key to optimise efficiency (Lentink and Biewener, 2010), (Hedenstrom et al., 2009). Unlike insects or birds, bats have heavy muscular wings with joints that enable higher degree of dexterity (Swartz et al., 2012).

This allows bats to save energy during flight than any other flying creature (Winter and Helversen, 1998), (Riskin et al., 2012). Also, their massive wings undergo large accelerations that are caused by inertial forces with a significant contribution for maneuvering (Iriarte-Diaz et al., 2011), (Riskin et al., 2010). This opens the path to a different way of attitude control for Micro Aerial Vehicles (MAV) that currently manoeuvre either by means of multiple rotating-propellers (like helicopters) or moving appendices such as flaps and rudders as in the case of fixed-wing MAV. In-

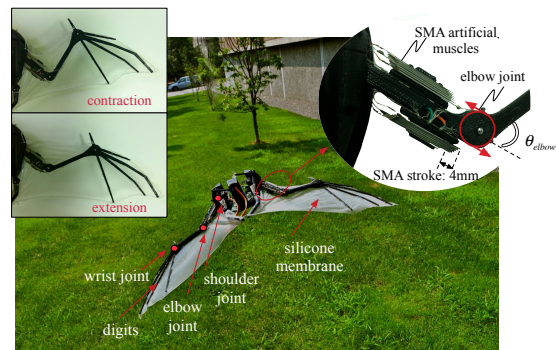


Figure 1: BaTbot, a bat-like morphing-wing MAV based on Bahlman et al., robotic wing design (Bahlman et al., 2013) but driven by Shape Memory Alloy (SMA) artificial muscles.

ertial forces are significant in bats because the mass of their wings comprise a significant portion of total body mass (large wing-to-body mass ratio) (Tholleson and Norberg, 1991).

Inspired by the morphology of the *Cynopterus brachiotus*, (Bahlman et al., 2013) proposed the de-

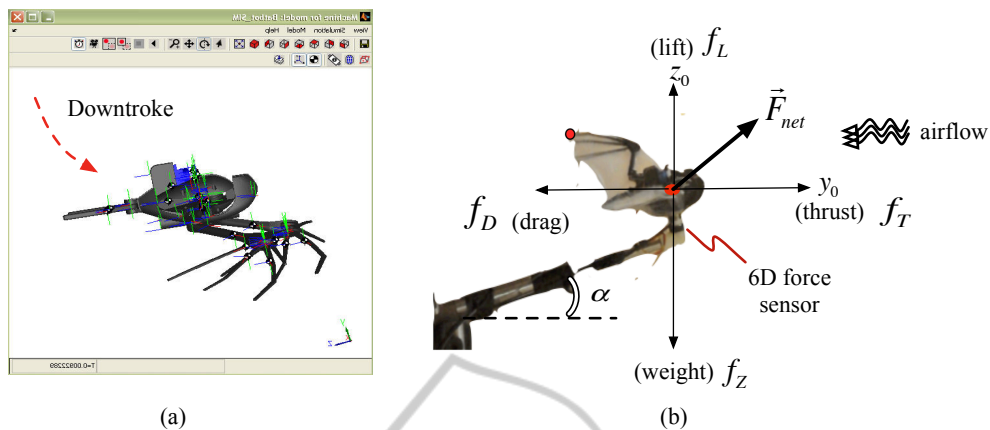


Figure 2: Lift, drag and thrust are measured as a function of the airflow speed ( $V_{air}$ ) and angle of attack ( $\alpha$ ); a) end of downstroke shown from the simulation dynamic-model, b) end of upstroke shown from the real setup.

sign of a multi-articulated wing structure from which the robotic model in Figure 1 was based. Results from (Bahlman et al., 2013) reported experimental measurements that detail the inertial and aerodynamic power involved in the cost of flapping and the contribution of the wing inertia in the overall cost of flight. Bahlman’s original wing design was modified in previous work (Colorado et al., 2012) so the robot could be actuated by Shape Memory Alloy (SMA) artificial muscles. Table 1 shows morphological parameters of BaTboT. Each wing of the robot has six degrees of freedom (dof): two-dof at the shoulder driven by a standard DC-motor, one-dof at the elbow driven directly by the SMA actuators, and three under-actuated dof at the wrist joint. The body is a six-dof floating base with rotations designated to roll, pitch and yaw following aerodynamic conventions. In this paper, we aim at identifying how to properly modulate the wing geometry for increasing net body forces ( $F_{net}$ ) that generate propulsion (Colorado et al., 2013) (cf. Figure 2b).

## 2 METHODS

Force measurements have been used for analysing the effects of applying different wing modulation patterns on lift generation, drag reduction and net body force production. By using data acquired with a wind-tunnel setup (Colorado et al., 2012; Colorado et al., 2013), our goal is to quantify how net body forces can be increased by changing the wing’s geometry in a proper way, using the morphing-wing mechanism presented in prior work (Colorado et al., 2012). To change the wing shape, we have used Nickel Titanium (NiTi) shape memory alloy actuators manufactured by *Migamotors* (cf. Figure 1). The very light struc-

Table 1: Morphological parameters.

Parameter [unit]	BaTboT
Total mass $m_t$ [g]	125
Extended wing length $B$ [m]	0.245
Body width $l_m$ [m]	0.04
Body mass $m_b$ [g]	18
Extended wingspan $S = l_m + 2B$ [m]	0.53
Extended wing area $A_b$ [m <sup>2</sup> ]	0.05
Humerus length $l_h$ [m]	0.055
Humerus average diameter $2r_h$ [m]	0.006
Radius length $l_r$ [m]	0.070
Radius average diameter $2r_r$ [m]	0.005
Wing mass <sup>1</sup> $m_w$ [g]	8.2
Membrane thickness [m]	0.0001

<sup>1</sup> Wing mass is composed by: humerus, radius, digits-III,IV,V and SMA actuators.

ture of the SMA actuators make them suitable for the construction of light wings with muscle-like actuation similar to the one found in bats. The morphing-wing mechanism is composed by an antagonistic pair of SMA actuators acting as artificial triceps and biceps muscles, which enable BaTboT to track bio-inspired wing motion trajectory patterns. More details regarding the SMA actuation mechanism can be found in (Colorado et al., 2012). Basically, the SMA act directly on the elbow joint ( $\theta_{elbow}$ ), thus enabling BaTboT to change its wingspan from 40.8cm (wings retracted) to 53cm (wings fully extended). As shown in the inset of Figure 1, the SMA actuators are connected to the elbow and wrist joints, allowing the wings to contract and extend at each wingbeat cycle. During the downstroke, wings are fully extended in order to maximise the area and increase lift, whereas during the upstroke, wings are folded in order to reduce drag. These modulation patterns for wing contraction and

extension are generated by applying a heating signal (electrical current) that activates the contraction stage of the SMA actuators.

To accelerate during forward flight, BaTboT must produce a net force to counteract gravity and overcome drag. As shown in Figure 2b, this force can be decomposed into a net force component in the direction of flight that corresponds to the difference between thrust ( $f_T$ ) and drag ( $D$ ), and a perpendicular component that corresponds to the difference between lift ( $L$ ) and weight ( $f_z$ ). Thus, net body forces can be calculated as:

$$F_{net} = (f_T - D) + (L - f_z), \quad (1)$$

In (1), both lift ( $L$ ) and drag ( $D$ ) force components depend on the angle of attack  $\alpha$  as shown in Figure 2b. Equation (2) shows these force components.

$$\begin{aligned} L &= f_L \cos(\alpha) - f_D \sin(\alpha) \\ D &= f_D \cos(\alpha) + f_L \sin(\alpha) \end{aligned} \quad (2)$$

### 3 RESULTS

*Could a Micro Aerial Vehicle (MAV) inspired by the biomechanics of bats take advantage of the morphing-wings aimed at increasing net body forces?* To test such hypothesis, we controlled the SMA actuators to apply three different morphing patterns for the wings, as shown in Fig. 3a. The plots show a close-up to a wingbeat cycle described by the elbow joint ( $\theta_{elbow}$ ). Such profiles differ in the proportion that the wing takes for contraction and extension during a wingbeat.

Firstly, we can note that the aerodynamic response is clearly affected by changing the wing modulation pattern. Figure 3b shows the lift ( $C_L$ ) and drag ( $C_D$ ) coefficients that correspond to each wing modulation pattern of column (a). Both coefficients have been calculated as:

$$\begin{aligned} C_L &= 2L(\rho V_{air}^2 A_b)^{-1}, \\ C_D &= 2D(\rho V_{air}^2 A_b)^{-1}, \end{aligned} \quad (3)$$

where  $\rho = 1.2(Kgm^3)$  is the air density,  $A_b = 0.05(m^2)$  is the wing area,  $L$  and  $D$  are the measured lift and drag forces at an angle of attack of  $\alpha = 10^\circ$ . We measured aerodynamic data using this configuration since the lift-to-drag ratio ( $L/D$ ) is maximum at that angle of attack (see the inset at the top plot of Fig. 3b). On average, the corresponding lift  $L$  and drag forces  $D$  are  $1.12N$  and  $0.112N$  respectively. These measurements correspond to the wing modulation pattern described by the top plot in Fig. 3a. Table 2 details the numerical values. *Despite keeping the same flapping frequency and airspeed within*

*the wind-tunnel*, note how lift and drag are affected after applying the wing profile described in both middle and bottom plots in Fig. 3a. The lift coefficient decreases whereas the drag coefficient increases depending on the angle of attack.

Similarly, net body force production is affected by changing the wing modulation patterns. We observed from the Fig. 3c that the upstroke portion of the wingbeat generates less drag due to the fact that the wing contracts sufficiently to reduce the area at minimum span. The experiments have confirmed that the generation of net body forces ( $F_{net}$ ) decreases when the wing modulation pattern is defined with equal proportions of contraction/extension during a wingbeat. The readings are even worst when the contraction during upstroke takes longer, as described by the bottom plots in Fig. 3.

To respond the question formulated at the beginning of this section, experimental results show that the contraction time of the wing (upstroke) should be faster than the extension time (downstroke), taking on average 37.5% of the wingbeat period. We performed extensive experiments with different wing modulation patterns; the three presented in Fig. 3a are the most representative of the studied cases. By comparing the bias of the net body forces between the middle and top plots of Fig. 3c, net body force production is increased by 28%. Table 2 summarises the numerical data corresponding to the experiments carried out in Fig. 3.

### 4 CONCLUSIONS

Our findings support the idea that by properly controlling the modulation of the wing geometry, more efficient flight can be achieved, just as bats efficiently generate net body forces taking advantage of their large wing-to-body mass ratio. In fact, we have demonstrated that with the proper wing kinematics, lift and net body forces can be increased whereas drag can be reduced. This leads to a significant increase in flight efficiency at the benefit of energy consumption. This approach opens the path to the development of novel attitude controllers (flight control) applied to flapping MAV, where the inertial forces produced by the wings are vital on the production of net body accelerations. The possibility of controlling the shape of the wings has great potential to improve the maneuverability of micro aerial vehicles for operating in confined spaces.

Table 2: Influence of wing modulation on flight performance.

Experiment	$\alpha(deg)$	$V_{air}(ms^{-1})$	$f(Hz)$	$C_L$	$C_D$	$\bar{L}(N)$	$\bar{D}(N)$	$f_z(N)$	$\bar{F}_{net}(N)$
Top	10	5	2–2.5	1.5	0.152	1.12	0.11	0.77	0.115
Middle	10	5	2–2.5	1.23	0.3	0.92	0.22	0.77	0.09
Bottom	10	5	2–2.5	0.48	0.17	0.36	0.12	0.77	0.021

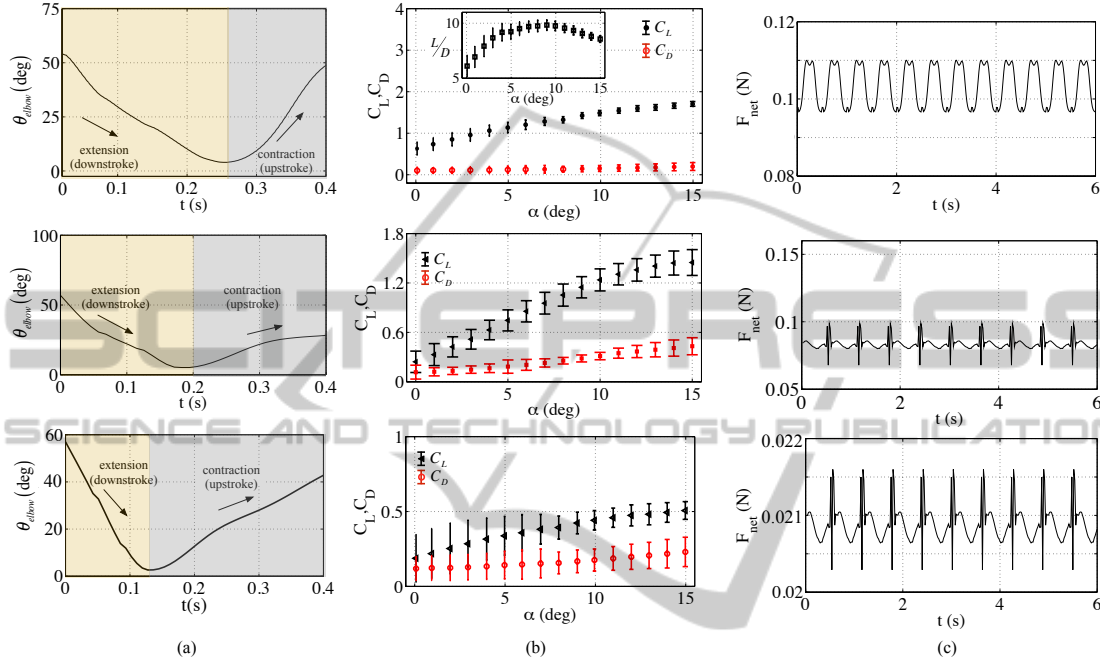


Figure 3: (Experimental) influence of wing modulation patterns ( $\theta_{elbow}$ ) on lift, drag and net body force production (airspeed of  $V_{air} = 5(ms^{-1})$  and wingbeat frequency of  $f = 2.5(Hz)$ ): a) close-up to a wingbeat with changes on wing modulation patterns, b) impact of changing wing modulation patterns from (a) on the lift coefficient  $C_L$  and the drag coefficient  $C_D$ , c) impact of changing wing modulation patterns from (a) on net body force production  $F_{net}$ .

## ACKNOWLEDGEMENTS

This work was supported by the Robotics and Cybernetics Group at Technical University of Madrid (Spain), and by the project entitled *Diseño y construcción de una plataforma robótica de exploración y reparación de tuberías hidrosanitarias, operada remotamente*, identifier 120350227348, funded by COLCIENCIAS y H&U. It was also funded by The Spanish Ministry of Education and Science (DPI2010-17998). The authors are thankful to professors Kenny Breuer and Sharon Swartz from Brown University for their knowledge about bat flight and for providing the wind-tunnel facility for the initials experiments carried out in (Colorado et al., 2012; Colorado et al., 2013). Furthermore, to Joe Bahlman from Brown University for the original design of the multi-articulated robotic wing used by BaTboT (Bahlman et al., 2013).

## REFERENCES

- Bahlman, J., Swartz, S., and Breuer, K. (2013). Design and characterization of a multi-articulated robotic bat wing. *Bioinspir. Biomim.*, (8):016009.
- Colorado, J., Barrientos, A., Rossi, C., Bahlman, J., and Breuer, K. (2012). Biomechanics of smart wings in a bat robot: morphing wings using sma actuators. *Bioinspir. Biomim.*, (7):036006.
- Colorado, J., Barrientos, A., Rossi, C., and Parra, C. (2013). Inertial attitude control of a bat-like morphing-wing air vehicle. *Bioinspir. Biomim.*, (8):016001.
- Gomez, J. and Garcia, E. (2011). Morphing unmanned aerial vehicles. *Smart Mater Struct.*, (20):1–16.
- Hedenstrom, A., Johansson, L., and Spedding, G. (2009). Bird or bat: comparing airframe design and flight performance. *Bioinspir. Biomim.*, vol. 4, no.1, pp. 5001.
- Iriarte-Diaz, J., Riskin, D., Willis, D., Breuer, K., and Swartz, S. (2011). Whole-body kinematics of a fruit bat reveal the influence of wing inertia on body accel-

- erations. *Journal of Experimental Biology*, vol. 214, no. 9, pp. 1546-1553.
- Lentink, D. and Biewener, A. (2010). Nature inspired flight-beyond the leap. *Bioinsp. Biomim*, vol. 5, no. 4, p040201.
- Riskin, D., Bergou, A., Breuer, K., and Swartz, S. (2012). Upstroke wing flexion and the inertial cost of bat flight. *Proceedings of the Royal Society B: Biological Sciences*, vol. 279, p2945-2950.
- Riskin, D., Iriarte-Diaz, J., Middleton, K., Breuer, K., and Swartz, S. (2010). The effect of body size on the wing movements of pteropodid bats, with insights into thrust and lift production. *The Journal of Experimental Biology*, vol. 213 (23) pp. 4110-4122.
- Swartz, S., Iriarte-Diaz, J., Riskin, D., and Breuer, K. (2012). A bird? a plane? no, its a bat: an introduction to the biomechanics of bat flight. *Evolutionary History of Bats Fossils, Molecules and Morphology*, p317-352, Cambridge.
- Thollessen, M. and Norberg, U. (1991). Moments of inertia of bat wings and body. *Journal of Experimental Biology*, vol. 158, 1991, pp. 19-35.
- Winter, Y. and Helversen, O. V. (1998). The energy cost of flight: do small bats fly more cheaply than birds? *J Comp Physiol B* 168: 105-111.